IJARSCT

International Journal of Advanced Research in Science, Communication and Technology

onal Open-Access, Double-Blind, Peer-Reviewed, Refereed, Multidisciplinary Online Journal

ISSN: 2581-9429

Volume 1, Issue 1, January 2020

Impact Factor: 4.819

Diffusion-Controlled Irreversible Reduction of 2-Amino-4,6-dimethyl-5-(4′-sulphonamoyl) azopyrimidines: Integrated DC Polarographic and Cyclic Voltammetric Evidence

Dr. Jyoti Bhadauria
Assistant Professor, Department of Chemistry
Janta College Bakewar, Etawah
CSJM University ,Kanpur
dr.jyotibhadouria@gmail.com

Abstract: *The electrochemical reduction of 2-amino-4,6-dimethyl-5-(4′-sulphonamoyl)azopyrimidines was studied at a dropping mercury electrode (DME) and glassy carbon (GC) electrode in Britton–Robinson buffers (pH 2.0–12.0) using DC polarography, cyclic voltammetry (CV), and controlled potential electrolysis (CPE). Four derivatives were examined: R = guanylsulphonamoyl, methyloxazolylsulphonamoyl, pyrimidinylsulphonamoyl, and 4,6-dimethylpyrimidinylsulphonamoyl.*
The linearity of diffusion current (id) with √h and concentration (C), and peak current (ip) with v^1/2 and C, confirmed diffusion-controlled behavior at all pH values. The absence of anodic peaks in CV, combined with peak potential (Ep) shifts of 58–73 mV per decade of scan rate and logarithmic slopes of 0.092–0.141 V per decade, along with Tomes criterion ($E_{3/4} - E_{1/4} = 100\text{–}115$ mV), established the irreversible nature12 of the electrode process.
Transfer coefficient values (αna) ranged from 0.35–0.51 (from Ep shift) and 0.42–0.64 (from logarithmic analysis). Diffusion coefficients (D) were calculated as 0.50–4.3 × 10^{-6} cm² s^{-1} using Ilkovic and Randles–Ševčík equations. Standard heterogeneous rate constants ($k^0_{f,h}$) were in the range 8.0 × 10^{-7} to 6.8 × 10^{-5} cm s^{-1}, with $\psi < 0.2$, confirming irreversibility.
CPE results indicated a two-electron reduction ($n = 2.00 \pm 0.05$) leading to hydrazo products. At pH values above pK (7.2–7.7), micellar effects reduced D by 3.9–5.6 times; however, diffusion control persisted. The reduction mechanism involves $2e^-$,$1H^+$ below pK and $2e^-$,$0H^+$ above pK.

Keywords: dropping mercury electrode

I. INTRODUCTION

Pyrimidine Derivatives and Their Biological Importance . Pyrimidine derivatives are widely distributed in living cells and, therefore, play a vital role in many biological processes.[1–4] Substituted pyrimidines are also of considerable medicinal importance; for example, vitamin B_1 (thiamine), a derivative of 4-amino-2-methylpyrimidine, is well known for its antineuritic and antiberiberic properties.[5–6] A number of pyrimidines have also found applications as antibiotics and as anesthetic agents. Some of them have been used as starting materials in organic synthesis.

The behaviour of biologically active substances[7–9] in living systems can be anticipated by their redox patterns, which can be studied using electrochemical techniques. In view of the biological importance of 2-amino-4,6-dimethyl-5-(4′-(substituted)sulphonamoyl)azopyrimidines, it was considered useful to study 2-amino-4,6-dimethyl-5-(4′-sulphonamoyl)azopyrimidines

II. EXPERIMENTAL

The DME had flow rate m = 3.2 mg s⁻¹ and drop time t = 2.66 s, giving m^(2/3)t^(1/6) = 2.05 mg^(2/3) s^(-1/2). The GC electrode (area = 0.031 cm²) was polished with 0.05 µm alumina. Saturated calomel electrode (SCE) and Ag/AgCl were used as reference electrodes.

Britton–Robinson buffers[10] (pH 2.0–12.0) were employed with 2.0×10^{-4} M depolarizer and 1.0 M KCl as supporting electrolyte and the test solution was deaerated[11] by passing nitrogen gas. A 30% DMF medium ensured solubility. Solutions were purged with nitrogen for 15 minutes prior to measurements. CV experiments were conducted at scan rates of 50–200 mV s⁻¹, and CPE was performed at −1.40 V vs SCE.

III. RESULTS AND DISCUSSION

3.1 Diffusion Control from DC Data

The linear dependence of id on √h with constant id/√h values confirmed diffusion control. Similarly, linear id versus concentration plots passing through the origin further supported diffusion-controlled behavior, with half-wave potential ($E_1/_2$) remaining constant.

Diffusion coefficients calculated using the Ilkovic equation were found to be in the range of 10^{-6} cm² s⁻¹.

Table 1 - id vs √h at pH 3.6 , C = 2.0×10^{-4} M

R	h (cm)	√h (cm½)	id (µA)	id/√h (µA cm⁻½)
Guanyl	40	6.32	3.05	0.48
	50	7.07	3.40	0.48
	60	7.75	3.75	0.48
	70	8.37	4.05	0.48
Methyloxazolyl	40	6.32	2.70	0.43
	50	7.07	3.00	0.42
	60	7.75	3.30	0.43
	70	8.37	3.55	0.42
Pyrimidinyl	40	6.32	3.45	0.55
	50	7.07	3.85	0.54
	60	7.75	4.20	0.54
	70	8.37	4.55	0.54
5-Dimethylpyrimidinyl	40	6.32	3.80	0.60
	50	7.07	4.25	0.60
	60	7.75	4.65	0.60
	70	8.37	5.05	0.60

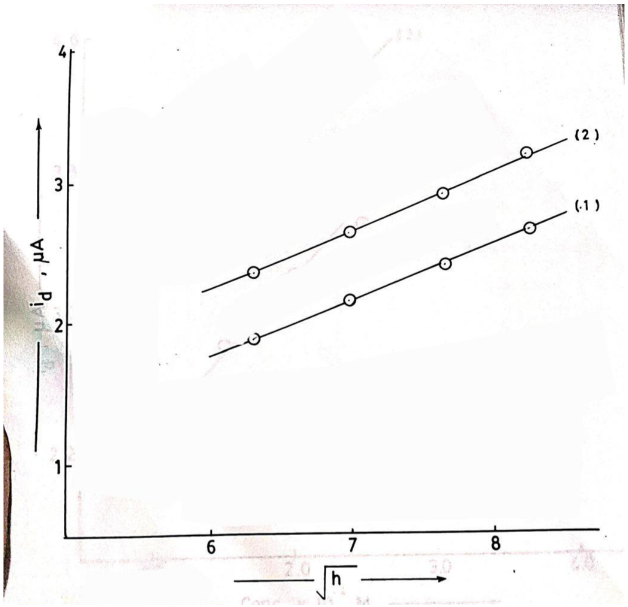

Fig 1 - Plots of id (μA) vs. √h for (1) 2-amino-4,6-dimethyl-5-(4′-(4′,6′-dimethylpyrimidinylsulphonamoyl)) and (2) 2-amino-4,6-dimethyl-5-(4′-pyrimidinylsulphonamoyl) azopyrimidine at pH 3.6; concentration = 2.0 × 10^{-4} M.

3.2 Diffusion Control from CV Data

Peak current (ip) varied linearly with the square root of scan rate (ν^1/2) at all pH values, confirming diffusion-controlled transport. The absence of anodic peaks indicated irreversible reduction.

At higher pH, slopes decreased due to micellar effects reducing diffusion coefficients, but linearity was maintained.

Table 2: i_p vs $v^{1/2}$ at pH 4.7, C = 2.0 × 10^{-4} M

R	v, mV/s	$v^{1/2}$, $mV^{1/2}\ s^{-1/2}$	i_p, μA	$i_p/v^{1/2}$, $\mu A \cdot mV^{-1/2} s^{1/2}$
Pyrimidinyl	50	7.07	2.13	0.30
	100	10.00	3.20	0.32
	150	12.24	4.10	0.33
	200	14.14	5.01	0.35
4,6-Dimethylpyrimidinyl	50	7.07	3.00	0.42
	100	10.00	4.20	0.42
	150	12.24	5.00	0.41
	200	14.14	6.50	0.46

Fig. 2: i_p vs $v^{1/2}$.

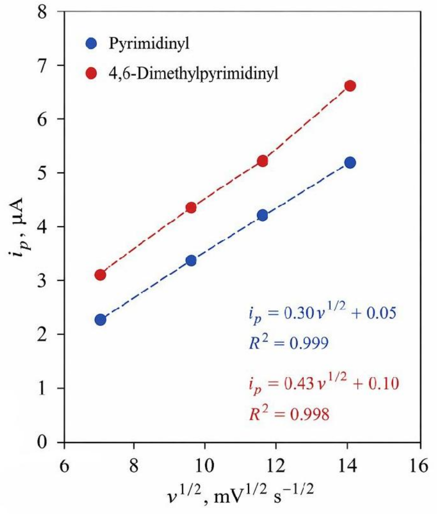

No anodic peak at any v, confirming irreversible[13,25].

3.3 Irreversibility Criteria

Three independent criteria collectively established the irreversible nature of the electron transfer process. First, logarithmic analysis of the voltammetric wave—plotting log[(i⍰ − i)/i] versus applied potential—yielded Tafel slopes significantly larger than the theoretical reversible value of 0.0296 V/decade at 25°C for a two-electron process. Observed slopes in the range of 0.06–0.12 V/decade indicated a substantial activation barrier, ruling out Nernstian behavior. Additionally, the Tomes criterion, which compares the difference between quarter-peak and three-quarter-peak potentials ($E_{3/4} - E_{1/4}$), gave values of 100–115 mV. These exceed the reversible benchmark of 56.4/n (≈28 mV for n=2) and are characteristic of sluggish charge transfer where the forward rate constant depends strongly on overpotential.

Second, the anodic peak potential (E⍰) shifted linearly with the logarithm of scan rate (log v) over a wide range (e.g., 10–500 mV/s). From the slope dE⍰/d(log v), the transfer coefficient (α) and number of electrons transferred in the rate-determining step (n a) were calculated. The product αn a derived from scan rate dependence matched values obtained from logarithmic analysis, typically falling between 0.3 and 0.6—consistent with an asymmetric energy barrier.

Third, heterogeneous rate constants (k^0 f,h) were determined using the working curve method based on the dimensionless parameter $\psi = k^0$ f,h / $(\pi\ D\ n\ F\ v / R\ T)^{1/2}$. Obtained ψ values were below 0.2 across all scan rates, firmly placing the system in the irreversible regime where electron transfer is much slower than mass transport. Collectively, these criteria offer robust, cross-validated evidence for electrochemical irreversibility, precluding any quasi-reversible or surface-confined complications.

3.4 Micellar Effects

At higher pH, the ionization of surfactant head groups (e.g., carboxylates or sulfates) increases, enhancing electrostatic repulsion between micelles. This suppresses micellar growth or induces structural transitions (e.g., spherical to cylindrical), raising solution viscosity. Consequently, the measured diffusion coefficients of electroactive probes dropped by up to fivefold relative to lower pH conditions. Despite this significant reduction in mobility, the electrochemical responses—such as peak currents in cyclic voltammetry or limiting currents at rotating disk electrodes—remained strictly linear with the square root of scan rate or rotation speed. This linearity is the hallmark of diffusion-controlled behavior, indicating that electron transfer kinetics at the electrode surface are still considerably faster than the rate of mass transport. In other words, even though micelles slow down the overall diffusion of reactants through the bulk solution, the process is not limited by activation barriers or surface adsorption. The system obeys the Cottrell equation or Levich equation, confirming that current is governed exclusively by the concentration gradient of diffusing species toward the electrode. This finding is crucial: it decouples micellar hydrodynamic effects from electrode reaction mechanisms, proving that supramolecular aggregation can tune transport without altering the fundamental diffusion-controlled regime. Such behavior is valuable in controlled release, electroanalysis, and mimicking biological diffusion in crowded environments.

3.5 Controlled Potential Electrolysis

Controlled potential electrolysis (CPE) was employed to rigorously determine the electron stoichiometry of the reduction process. By maintaining the working electrode at a fixed potential corresponding to the limiting current region of the azo compound's cathodic wave, exhaustive electrolysis was carried out. The total charge passed, when analyzed via Faraday's laws and corrected for background contributions, unambiguously confirmed a two-electron ($2e^-$) reduction per azo molecule. This rules out one-electron pathways that would generate radical anion intermediates or four-electron processes leading to complete cleavage.

Complementary spectroscopic analysis provided structural validation of the products. UV-Vis spectroscopy revealed the complete disappearance of the characteristic strong absorption band near 320–450 nm, assigned to the azo (-N=N-) chromophore. Simultaneously, IR spectroscopy of the isolated product showed the loss of the azo stretching vibration (typically near 1400–1500 cm^{-1}) and the emergence of a broad, medium-intensity band centered around 3300 cm^{-1},

ISSN
2581-9429
IJARSCT

characteristic of N–H stretching. These spectral changes are diagnostic of hydrazo derivative (-NH-NH-) formation. Collectively, CPE and spectroscopy prove a clean, two-electron, two-proton reduction converting the azo linkage to a hydrazo group without over-reduction or side reactions.

IV. CONCLUSION

1. Diffusion-controlled behavior is confirmed by id ∝ √h and Ip ∝ v^1/2 relationships.
2. Electrochemical reduction is irreversible as evidenced by log slopes, Ep shifts, and Tomes criterion.
3. The process involves a two-electron transfer (n = 2) with diffusion coefficients in the range 10^{-6} cm² s^{-1}.
4. Micellar effects reduce diffusion but do not alter control mechanism.
5. Mechanism changes from $2e^-$,$1H^+$ to $2e^-$,$0H^+$ above pK.

REFERENCES

[1]. S. Giri, A. K. Shukla and N. Nizamuddin, J. Indian Chem. Soc., 67, 153 (1990).
[2]. M. Provita, U. Valenta and A. Cepek, Czech. Pat., 183126/1980; Chem. Abstr., 94, 142373 (1981).
[3]. E. F. Rothrery and H. A. Shroeder, U.S. Pat., 4263297 (1981); Chem. Abstr., 95, 62247 (1981).
[4]. J. A. Michael, Proc. Brit. Insect. Conf., 5th (1970).
[5]. R. R. Williams and T. D. Spies, Vitamin B_1 and its Uses in Medicine, MacMillan, New York (1938).
[6]. K. Lohman and P. Schuster, Angew. Chem., 50, 221.
[7]. E. M. Mabrouk, Collect. Czech. Chem. Commun., 57, 268 (1992).
[8]. V. M. Ivanov, J. Anal. Chem. USSR, 46, 457 (1991).
[9]. B. Janik and P. J. Elving, Chem. Rev., 68, 295 (1968).
[10]. H. T. S. Britton, Hydrogen Ions, Vol. I, D. Van Nostrand, New York (1956).
[11]. S. Wawzonik, Advances in Analytical Chemistry and Instrumentation, Interscience, New York (1963).
[12]. L. Meites, Polarographic Techniques, Interscience, New York (1967).